JAERI-M
82-080

MATRIX METHOD FOR KINETIC BALLOONING MODE

July 1982

Shinji TOKUDA, Kimitaka ITOH, Takashi TUDA
and Sanae-Inoue ITOH*

日本原子力研究所
Japan Atomic Energy Research Institute

JAERI-M レポートは，日本原子力研究所が不定期に公刊している研究報告書です。
入手の問合わせは，日本原子力研究所技術情報部情報資料課（〒319－11 茨城県那珂郡東海村）あて，お申しこしください。なお，このほかに財団法人原子力弘済会資料センター（〒319－11 茨城県那珂郡東海村日本原子力研究所内）で複写による実費頒布をおこなっております。

JAERI-M reports are issued irregularly.
Inquiries about availability of the reports should be addressed to Information Section, Division of Technical Information, Japan Atomic Energy Research Institute, Tokai-mura, Naka-gun, Ibaraki-ken 319—11, Japan.

編集兼発行　日本原子力研究所
印　　刷　日立高速印刷株式会社

JAERI-M 82-080

Matrix Method for Kinetic Ballooning Mode

Shinji TOKUDA, Kimitaka ITOH, Takashi TUDA and Sanae-Inoue ITOH*

Division of Thermonuclear Fusion Research,

Tokai Research Establishment, JAERI

(Received June 11, 1982)

A matrix method is developed to solve numerically the kinetic high-n ballooning mode. This method approximates directly the difference - differential equation by a finite difference method. Toroidal mode coupling effects and full electron and ion responses are described in the correct forms. Performance, convergence property and accuracy of the method are investigated.

Keywords: Kinetic Ballooning Mode, Toroidal Plasma,
Difference-Differential Equation, Finite Difference Method,
Matrix Renumbering, Newton's Method, Contour Map.

---

*) Institute for Fusion Theory, Hiroshima University

JAERI－M 82－080

運動論的バルーニング・モードの行列法解法

日本原子力研究所東海研究所核融合研究部
徳田　伸二・伊藤　公孝・津田　　孝
伊藤　早苗*

（1982年6月11日受理）

高モード数の運動論的バルーニング・モードを数値的に解く行列法を開発した。この方法は，差分－微分方程式を差分法で直接近似する。トロイダル効果および電子やイオンの応答が正しい形で表現される。この方法の性能，収束性および精度を調べた。

*）広島大学核融合理論研究センター

Contents

目　　次

1. Introduction

We have recently reported on electrostatic[1] and electromagnetic[2] drift wave ballooning instabilities in toroidal plasmas by means of the matrix method to solve the difference - differential equations of the high n ballooning modes. In this paper, we present the detailed description of the matrix method, and report on performance, convergence property and accuracy of the method. This paper is mainly concerned with the equation which describes the electrostatic ballooning mode. However, our method can be applied to the ballooning modes which retained the trapped particle effects as well as the electromagnetic drift wave ballooning mode with the straight forward extentions.

The perturbed potential, $\tilde{\phi}(\vec{r},t)$, of the elctrostatic drift wave ballooning mode is described by the equations[3]

$$\tilde{\phi}(\vec{r},t) = \sum_m \phi_m(r)\exp(-i\omega t + im\theta - i\ell\varphi)$$

$$\{\frac{d^2}{dx^2} - k^2\rho_i^2 + P(x)\}\phi_m(x) = \frac{\varepsilon\omega_*}{\tau\omega}\{(1-\frac{1}{k\rho_i}\frac{d}{dx})\phi_{m-1}(x) + (1+\frac{1}{k\rho_i}\frac{d}{dx})\phi_{m+1}(x)\}, \quad (1.1)$$

$$P(x) = \frac{1}{2\xi_i Z(\xi_i)}\{\frac{\omega_* - \omega}{\omega\tau+\omega_\kappa} Z'(\xi_e) - Z'(\xi_i)\} \quad (1.2)$$

in the (r,θ,φ) coordinate system (θ,φ are poloidal and toroidal angles). In Eqs.(1), the following notations are used : $x = (r-r_s)/\rho_i$, $q(r_s) = m/\ell$, $k = m/r$, $\xi = \omega/(\sqrt{2}|k_\parallel|v_t)$, $k_\parallel = (m-\ell q)/(qR)$, $\tau = T_e/T_i$, $\omega_* = cT_e k/(eBL_n)$, $\kappa = 1/L_n = dn_0/dr\ /n_0$, $\varepsilon = L_n/R$ and Z is the plasma dispersion function. Other notations are standard. The right hand side of Eq.(1.1) denotes the mode coupling due to toroidal effects. The high - ℓ ($\ell \gg 1/\varepsilon$) ballooning mode approximation reduces the set of coupled differential equations (1.1) to a one dimensional difference - differential equation[3]

$$\{\frac{d^2}{dx^2} - k^2\rho_i^2 + P(x)\}\phi(x) = \frac{\varepsilon\omega_*}{\tau\omega}\{(1 - \frac{1}{k\rho_i}\frac{d}{dx})\phi(x+\Delta) + (1 + \frac{1}{k\rho_i}\frac{d}{dx})\phi(x-\Delta)\} \quad (2)$$

with $\phi_j(x) = \phi(x-j\Delta)$ where $\Delta = 1/(k\rho_i s)$ $(s=rq'/q)$, $j = m-m_0$, and x is redefined as $q(x=0) = m_0/\ell$. We concerned on solving Eq.(2) numerically. This is one of the generalized eigenvalue problem with the boundary condition, $\phi(x) \to 0$ as $|x| \to \infty$. Several numerical methods have been used to solve Eq.(2). The weak and strong coupling approximation[3,4,5,6] limit the available parameter regions of the analyses. The Fourier decomposing ballooning representation[7,8,9,10,11] has difficulty in including the correct forms of electron andion responses. The drift wave theory in a slab model has clarified that the wave is stabilized by magnetic shear and the correct treatment of electron response is important to dictate the stability[12,13]. The method treated by this paper is a finite difference method which approximates directly Eq.(2). Therefor, the mode coupling effect and the full electron and ion responses are kept in correct forms. The finite difference method reduces the eigenvalue problem of the difference - differential equation to that of a linear equation. It is solved by three procedures ;

(1) matrix renumbering to save CPU time and Core Memory,

(2) contour map to seek the eigenvalues, and

(3) Newton's method to obtain them by iteration.

In Sec.2, we describe the method in detail, In Sec.3, we investigate the performance, convergence property and accuracy of the method. Summary and discussion are given in Sec.4.

2. Numerical Method

2.1 Matrix Formulation

The derivatives that appear in Eq.(2) are approximated by

$$\{\frac{d^2}{dx^2} - k^2\rho_i^2 + P(x)\}\phi(x) = \frac{\varepsilon\omega_*}{\tau\omega}\{(1 - \frac{1}{k\rho_i}\frac{d}{dx})\phi(x+\Delta) + (1 + \frac{1}{k\rho_i}\frac{d}{dx})\phi(x-\Delta)\} \quad (2)$$

with $\phi_j(x) = \phi(x-j\Delta)$ where $\Delta = 1/(k\rho_i s)$ $(s=rq'/q)$, $j = m-m_0$, and x is redefined as $q(x=0) = m_0/\ell$. We concerned on solving Eq.(2) numerically. This is one of the generalized eigenvalue problem with the boundary condition, $\phi(x) \to 0$ as $|x| \to \infty$. Several numerical methods have been used to solve Eq.(2). The weak and strong coupling approximation[3,4,5,6] limit the available parameter regions of the analyses. The Fourier decomposing ballooning representation[7,8,9,10,11] has difficulty in including the correct forms of electron andion responses. The drift wave theory in a slab model has clarified that the wave is stabilized by magnetic shear and the correct treatment of electron response is important to dictate the stability[12,13]. The method treated by this paper is a finite difference method which approximates directly Eq.(2). Therefor, the mode coupling effect and the full electron and ion responses are kept in correct forms. The finite difference method reduces the eigenvalue problem of the difference - differential equation to that of a linear equation. It is solved by three procedures ;

(1) matrix renumbering to save CPU time and Core Memory,

(2) contour map to seek the eigenvalues, and

(3) Newton's method to obtain them by iteration.

In Sec.2, we describe the method in detail, In Sec.3, we investigate the performance, convergence property and accuracy of the method. Summary and discussion are given in Sec.4.

2. Numerical Method

2.1 Matrix Formulation

The derivatives that appear in Eq.(2) are approximated by

$$\frac{d}{dx}\phi\Big|_j = \frac{\phi_{j+1} - \phi_{j-1}}{2h} \quad , \quad \frac{d^2}{dx^2}\phi\Big|_j = \frac{\phi_{j+1} - 2\phi_j + \phi_{j-1}}{h^2}$$

introducing even mesh $x_j = jh$ (j=0, +1, +2, ...). Then the finite difference approximation of Eq.(2) is given by

$$\begin{aligned} &\frac{\varepsilon\omega_*}{\tau\omega}\left(-\frac{1}{k\rho_i}\frac{h}{2}\phi_{j-n-1} + h^2\phi_{j-n} + \frac{h}{2}\frac{1}{k\rho_i}\phi_{j-n+1}\right) \\ &- \phi_{j-1} + \left(2 + h^2k^2\rho_i^2 - h^2P_j \right)\phi_j - \phi_{j+1} \\ &+ \frac{\varepsilon\omega_*}{\tau\omega}\left(\frac{1}{k\rho_i}\frac{h}{2}\phi_{j+n-1} + h^2\phi_{j+n} - \frac{h}{2}\frac{1}{k\rho_i}\phi_{j+n+1}\right) = 0 \quad , \quad (3) \end{aligned}$$

where $n = \Delta/h$ and $P_j = P(x_j)$. The boundary condition of the solution are $\phi(x) \to 0$ as $|x| \to \infty$. Therefore the system of Eq.(3) is truncated at $x_N = hN$ where the solution $\phi(x)$ exponentially damps off. Eq.(2) conservs the parity ; $\phi(-x) = \phi(x)$ (even mode) or $\phi(-x) = -\phi(x)$ (odd mode). Noticing this fact, we can rewrite Eq.(3) in a matrix form

$$A \begin{pmatrix} \phi_0 \\ \phi_1 \\ \vdots \\ \phi_N \end{pmatrix} = 0 \qquad (4)$$

and the matrix A has the following structure ;

$$A = (a_{i,j}) = \begin{bmatrix} & & & & \\ & & & & \\ & & & & \\ & & & & \\ & & & & \end{bmatrix} \qquad (5)$$

where tridiagonal terms arise form d^2/dx^2 and the slab potential and off-diagonal temrs appear for $j = i \pm n$, $i \pm n + 1$ and $i \pm n - 1$ due to

the toroidal coupling. The (i, j) = (i, n - i), (i, n - i ± 1) elements arise from the parity. The eigenvalue ω is determined by the equation

$$D(\omega) = \det(A) = 0 \tag{6}$$

which is the necessary and sufficient condition that Eq.(4) has non trivial solution.

2.2 Newton's Method and Matrix Renumbering

Eq.(6) needs to be solved by iteration because $D(\omega)$ is a transcendental function of ω. We adopt Newton's method in which $dD/d\omega$ is approximated as

$$\frac{D(\omega_1) - D(\omega_2)}{\omega_1 - \omega_2}$$

where ω_1 and ω_2 are close to the solution $D(\omega) = 0$. Then the better approximation of the true solution ω_0 is given by

$$\omega_3 = \omega_2 - \frac{D(\omega_2)(\omega_2-\omega_1)}{D(\omega_2)-D(\omega_1)} \quad . \tag{7}$$

This argorithm works quite well as long as the start value of the iteration is close enough to ω_0 because $D(\omega)$ is a regular function of ω near the zero point of it. We plot contours of zeros of $\mathrm{Re}D(\omega)$ and $\mathrm{Im}D(\omega)$ on Re ω - Im ω plane. A crossing point can be taken as the start value of the iteration. Moreover this contour map reveals much more informations. When ω_0 is a single zero of D, i.e., $D(\omega) \sim C(\omega - \omega_0)$, then the lines $\mathrm{Re}D(\omega) = 0$ and $\mathrm{Im}D(\omega) = 0$ cross with 90°. For degenerate case, i.e., $D(\omega) \sim C(\omega - \omega_0)^2$, two lines of $\mathrm{Re}D(\omega) = 0$ and two lines of $\mathrm{Im}D(\omega) = 0$ cross with 45°. The most important is that the crossing of the lines $\mathrm{Re}D(\omega) = 0$ and $\mathrm{Im}D(\omega) = 0$ ensures the existence of the solution. If one plots contours of $|D(\omega)|$, the absolute value of $D(\omega)$, many minimal points will appear ; some of them coinside true solutions and some are not. The

accumulation of the numerical error will prevent $|D(\omega)|$ from vanishing. These difficulties are resolved by the contour method.

The LDU decomposition of the matrix A is used to compute $D(\omega)$, where L and U are unit lower and upper triangular matrices and D a diagonal matrix. The determinant $D(\omega)$ is given by the multiplication of all the diagonal elements of D. It is natural to use Time Sharing System (TSS) in order to solve Eq.(6) by Newton's method. TSS limits CPU time and Core Memory while Newton's method requires to compute $D(\omega)$ many times. It is not sufficient for saving CPU time and Core Memory only to take advantage of the band structure of the matrix A. We can make the matrix A narrower by means of permutation of unknowns. This technique is known as 'Renumbering of matrix'[14]. Let us consider 20X20 matrix of n = 15. This is a band matrix with 15 half band width as shown in Fig.(1.a). We renumber the unknowns by post-order rule as ;

$$(1) \rightarrow 1,\ (16) \rightarrow 2,\ (15) \rightarrow 3,\ (14) \rightarrow 4,$$
$$(2) \rightarrow 5,\ (17) \rightarrow 6,\ (3) \rightarrow 7,\ (13) \rightarrow 8,\ \ldots$$

Fig.(1.b) shows the graphical representation of our rule. After renumbering, as shown in Fig.(1.c), the matrix A is exchanged into a matrix with 5 half band width. This is a simple effective argorithm to renumber the matrix A for arbitrary n. In Fig.(2), we show the band width M_A after renumbering as a function of the band width M_o of the 200 × 200 matrix. The dotted line is $M_A = M_o$. Renumbering is profitable for $M_A \geqq 50$. Moreover, it has attractive feature that the larger M_o is, the narrower the renumbered matrix becomes. This feature is crucial for the matrix method to succeed. Figs.(3) show the necessary Core Memory (byte) and CPU time (s) to compute $D(\omega)$ by FACOM M-200 in JAERI as a function of the mesh size h ($h_M = h/(\kappa L_s)$) when truncation length $Nh = \kappa L_s$ is fixed. I and II are the cases of LDU decomposition without and with use of the band structure, respectively.

III indicates the case of the renumbered matrix. The upper limit of Core Memory for our TSS system is shown in Fig.(3.a). We also show in Fig.(3.c) the convergence curves of real and imaginary parts of ω and mesh sizes to get 'good convergence' (see Fig.8); the parameters are $q = 1$, $k\rho_i = 0.1$, $\tau = 1$, $s = 1$, $\varepsilon = 0.1$. Renumbering is indispensable to solve Eq.(6) with high accuracy by TSS and under the IN - CORE condition. Reduction of CPU time due to renumbering enables us to investigate the solution of Eq.(2) over the extensive parameter space.

3. Property of the Matrix Method

The matrix method to obtain numerically the eigenvalue of Eq.(2) needs convergence study. We can get only the eigenvalue ω of Eq.(3). This is a function of the mesh size h, i.e., $\omega = \omega(h)$. The true eigenvalue of Eq.(2) is given by the limit of $\omega(h)$ when $h \to 0$. This limit can be obtained by extrapolating the convergence curve of $\omega(h)$.

The fluid limit of Eq.(2) can be solved by the shooting method with the help of Fourier transformation. In this section, for the case of the fluid limit, we first investigate the convergence property and accuracy of the matrix method by comparison with the shooting method. Next, we give the convergence study for the general case of Eq.(3).

3.1 Comparison with Shooting Method

Eq.(2) can be solved by the shooting method in the fluid limit. Replacing the electron response with Boltzmann response and expanding the ion Z function as $Z'(\xi_i) \simeq 1/\xi_i^2$, we get the approximation of Eq.(2) ;

$$\frac{d^2\phi}{dx^2} + \left[-k^2\rho_i^2 + \frac{\omega_* - \omega}{\omega\tau + \omega_*} + \frac{(1+\tau)\omega_*^2}{(\tau\omega+\omega_*)\omega} \frac{k_{//}^2 v_i^2}{\omega^2} \right] \phi(x)$$
$$= \frac{\varepsilon\omega_*}{\tau\omega} \left[\left(1 - \frac{1}{k\rho_i}\frac{d}{dx}\right) \phi(x+\Delta) + \left(1 + \frac{1}{k\rho_i}\frac{d}{dx}\right) \phi(x-\Delta) \right] . \qquad (8)$$

This can be solved by use of the matrix method. In this case, however, the

III indicates the case of the renumbered matrix. The upper limit of Core Memory for our TSS system is shown in Fig.(3.a). We also show in Fig.(3.c) the convergence curves of real and imaginary parts of ω and mesh sizes to get 'good convergence' (see Fig.8); the parameters are $q = 1$, $k\rho_i = 0.1$, $\tau = 1$, $s = 1$, $\epsilon = 0.1$. Renumbering is indispensable to solve Eq.(6) with high accuracy by TSS and under the IN - CORE condition. Reduction of CPU time due to renumbering enables us to investigate the solution of Eq.(2) over the extensive parameter space.

3. Property of the Matrix Method

The matrix method to obtain numerically the eigenvalue of Eq.(2) needs convergence study. We can get only the eigenvalue ω of Eq.(3). This is a function of the mesh size h, i.e., $\omega = \omega(h)$. The true eigenvalue of Eq.(2) is given by the limit of $\omega(h)$ when $h \to 0$. This limit can be obtained by extrapolating the convergence curve of $\omega(h)$.

The fluid limit of Eq.(2) can be solved by the shooting method with the help of Fourier transformation. In this section, for the case of the fluid limit, we first investigate the convergence property and accuracy of the matrix method by comparison with the shooting method. Next, we give the convergence study for the general case of Eq.(3).

3.1 Comparison with Shooting Method

Eq.(2) can be solved by the shooting method in the fluid limit. Replacing the electron response with Boltzmann response and expanding the ion Z function as $Z'(\xi_i) \simeq 1/\xi_i^2$, we get the approximation of Eq.(2) ;

$$\frac{d^2\phi}{dx^2} + \left[-k^2\rho_i^2 + \frac{\omega_* - \omega}{\omega\tau + \omega_*} + \frac{(1+\tau)\omega_*^2}{(\tau\omega+\omega_*)\omega} \frac{k_{//}^2 v_i^2}{\omega^2} \right] \phi(x)$$
$$= \frac{\epsilon\omega_*}{\tau\omega} \left[\left(1 - \frac{1}{k\rho_i}\frac{d}{dx}\right) \phi(x+\Delta) + \left(1 + \frac{1}{k\rho_i}\frac{d}{dx}\right) \phi(x-\Delta) \right] . \qquad (8)$$

This can be solved by use of the matrix method. In this case, however, the

slab potential is of the form as $C_1+C_2x^2$, and therefor the eigenvalue is obtained alternatively by Fourier transform and the shooting method. Eq(8) can be rewitten as the ordinary differential equation ; ($k_\eta = kx/L_s$)

$$\frac{d^2\psi}{d\eta^2} - \frac{\omega(\tau\omega+\omega_*)\tau^2}{(1+\tau)\omega_*^2}(\kappa L_s)^2\left[\frac{\omega_*-\omega}{\omega\tau+\omega} - k^2\rho_i^2 - \eta^2 + \frac{2\varepsilon\omega_*}{\tau\omega}(\cos\Delta\eta + s\Delta\eta\sin\Delta\eta)\right]\psi = 0 \qquad (9)$$

where $\phi(x) = \int_{-\infty}^{\infty}\psi(\eta)e^{i\eta x}dx$. Since we look for the solution which is localized in x space, Eq.(9) is solved with the boundary condition that $\psi(\eta)$ damps off as $|\eta| \to \infty$. The parity of $\psi(\eta)$ is the same as that of $\phi(x)$. We can solve Eq.(9) numerically by means of the shooting method. Comparing the eigenvalue and eigensolution computed from the two different methods, we can confirm the validity of the matrix method.

Fig.(4.a) shows the convergence curve of eigenvalue computed by the matrix method for the parameters ; $s = 1$, $k\rho_i = 0.2$, $q = 3.2$, $\tau = 1$, $\varepsilon = 0.1$, $\Delta = 5$ and $\kappa L_s = 32$. The truncation length is fixed as $Nh = \kappa L_s$. The eigenvalue given by the shooting method is $\omega = (0.2658248, 0.3691862)\,\omega_*$. The convergence is quadratic for $1/h$ with positive gradient for $\omega = Re(\omega)$ and negative for $\gamma = Im(\omega)$. The extrapolate values of them accord with those for the shooting method with very high accuracy. Fig.(4.b) shows the convergence curve when the truncation length N is varied and the mesh size h is fixed to $h = 0.0104\,\kappa L_s$. For $N \geq 80$, the eigenvalue computed by the matrix method converges to that computed by the shooting method. If $N < 60$, the eigenvalue fluctuates rapidly because the eigensolution does not still damp of at $x = Nh$.

Fig.(5) illustrates the eigensolution obtained by the shooting method. The solid and dotted line indicate the real and imaginary parts of the solution, respectively. We show $\psi(\eta)$ in Fig.(5.a) and its Fourier transform, $\phi(x)$ in Fig.(5.b). We also show in Fig.(6) the eigensolution

by the matrix method for $h = 2.2 \times 10^{-2} \kappa L_s$ (Fig.(6.a)) and $h = 5.04 \times 10^{-3} \kappa L_s$ (Fig.(6.b)). The eigensolution $\phi(x)$ for $h/(\kappa L_s) = 5.04 \times 10^{-3}$ is in good accordance with that by the shooting method. Therefore we conclude that the matrix method works quite satisfactory.

The shooting method with Fourier transformation cannot be applied when the slab potential has not the form of a polynomial function of x as Eq.(9) but has the general form. On the other hand, the matrix method can solve Eq.(2) including the correct form of $P(x)$, which is the character of the matrix method.

3.2 Convergence for the General Case

The contour map gives good starting values of iteration. Fig.(7) shows an example of contour map (parameters are : $q = 3.2$, $k\rho_i = 0.2$, $\tau = 1$, $s = 1$ and $\varepsilon = 0.1$.) The solid and dotted lines indicate Re $D(\omega) = 0$ and Im $D(\omega) = 0$, respectively. There are many crossing points, i.e., the solutions of $D(\omega) = 0$. they can be used as the starting value. The contour map gives more information about the solution. We can classify the solution into several branches[1] by studying the structure of eigensolution $\phi(x)$ and the parameter dependence of the trajectory of the eigenvalue in the Reω - Im ω plane. For example, the solution A is the Perlstein - Berk branch which is stable in the slab limit ($\varepsilon \to 0$). It is almost stable in the toroidal geometry over various parameters. The most unstable solution C belongs to the other branch which has localized structure and highly stable in the slab limit. The solution B is not a higher mode belonging to the same branch as C, but the foundamental localized solution of the toroidicity - induced branch. It approaches $(\omega, \gamma) \longrightarrow (0, 0)$ as $\varepsilon \longrightarrow 0$.

Fig.(8) shows the convergence curve of the eigenvalue belonging to the C branch, where the parameters are : $q = 5$, $k\rho_i = 0.2$, $\tau = 1$, $s = 1$ and

$\varepsilon = 0.1$. We also illustrate the eigensolutions for $h = 10^{-2}\ \kappa L_s$ (Fig.(9.a)) and for $h = 0.25 \times 10^{-2}\ \kappa L_s$ (Fig.(9.b)). The point A in Fig.(8) denotes such a mesh size as $k_{\parallel}(h_A)v_e/\omega \simeq 1/4$ and B denotes $k_{\parallel}(h_B)v_e/\omega \simeq 1/2$. If the mesh size is smaller than h_A, i.e., the potential due to the electron response is described enough accurately, the convergence curve is quadratic. Therefore, the extrapclated eigenvalue is assured to be the true value. For larger meshes than h_B the convergence curve derivates from quadratic. However, we can get accurate eigenvalue and eigensolution (see Fig.(9)) for those meshes. Even for $h/(\kappa L_s) \simeq 10^{-2}$, The eigenvalue approximates to the extrapolated value within the error $\lesssim 1$ % .

4. Summary and Discussions

We have presented a matrix method to solve numerically the difference-differential equation of the electrostatic high-n ballooning mode. It approximates directly the equation using the finite difference method. Then the toroidal mode coupling effects and the electron and ion responses are kept in the correct forms. The generalized eigenvalue problem is reduced to that of a linear equation, which is solved by three procedures, that is, (1) matrix renumbering to save CPU time and Core Memory, (2) contour map to seek eigenvalues, and (3) Newton's method to obtain them by iteration. We have investigated the performance, convergence property and accuracy of the matrix method in detail. The convergence of eigenvalues is shown to be quadratic for fine meshes. This method gives accurate solution and enables us to study the high-n ballooning modes over the extensive parameter space by TSS and under IN-CORE condition.

The matrix method can be applied to the electromagnetic ballooning mode. For this case, the matrix becomes a matrix which has the seven width band structure in the slab and mode coupling terms. Then, no changes need in

$\varepsilon = 0.1$. We also illustrate the eigensolutions for $h = 10^{-2}\ \kappa L_s$ (Fig.(9.a)) and for $h = 0.25 \times 10^{-2}\ \kappa L_s$ (Fig.(9.b)). The point A in Fig.(8) denotes such a mesh size as $k_{\prime\prime}(h_A)v_e/\omega \simeq 1/4$ and B denotes $k_{\prime\prime}(h_B)v_e/\omega \simeq 1/2$. If the mesh size is smaller than h_A, i.e., the potential due to the electron response is described enough accurately, the convergence curve is quadratic. Therefore, the extrapclated eigenvalue is assured to be the true value. For larger meshes than h_B the convergence curve derivates from quadratic. However, we can get accurate eigenvalue and eigensolution (see Fig.(9)) for those meshes. Even for $h/(\kappa L_s) \simeq 10^{-2}$, The eigenvalue approximates to the extrapolated value within the error $\lesssim 1$ % .

4. Summary and Discussions

We have presented a matrix method to solve numerically the difference-differential equation of the electrostatic high-n ballooning mode. It approximates directly the equation using the finite difference method. Then the toroidal mode coupling effects and the electron and ion responses are kept in the correct forms. The generalized eigenvalue problem is reduced to that of a linear equation, which is solved by three procedures, that is, (1) matrix renumbering to save CPU time and Core Memory, (2) contour map to seek eigenvalues, and (3) Newton's method to obtain them by iteration. We have investigated the performance, convergence property and accuracy of the matrix method in detail. The convergence of eigenvalues is shown to be quadratic for fine meshes. This method gives accurate solution and enables us to study the high-n ballooning modes over the extensive parameter space by TSS and under IN-CORE condition.

The matrix method can be applied to the electromagnetic ballooning mode. For this case, the matrix becomes a matrix which has the seven width band structure in the slab and mode coupling terms. Then, no changes need in

the basic procedures of the method and we can compact the matrix by suitable renumbering.

ACKNOWLEDGEMENTS

The authors wish to thank the members of the theory group of JAERI for useful helps and discussions. They are also grateful to Drs. T. Takeda, M. Tanaka and Y. Obata for continuous encouragements. One of the authors (S.I.I) shows sincere gratitudes to Dr. Y. Obata for hospitalities.

the basic procedures of the method and we can compact the matrix by suitable renumbering.

ACKNOWLEDGEMENTS

The authors wish to thank the members of the theory group of JAERI for useful helps and discussions. They are also grateful to Drs. T. Takeda, M. Tanaka and Y. Obata for continuous encouragements. One of the authors (S.I.I) shows sincere gratitudes to Dr. Y. Obata for hospitalities.

References

1] K. Itoh, T. Tuda, S. Tokuda and S.-I. Itoh, Japanese J. Appl. Phys. 20 (1981) L801.

2] T. Tuda, K. Itoh, S. Tokuda and S.-I. Itoh, Controlled Fusion Conference (Austin, 1981), and K.Itoh, S.-I. Itoh, S. Tokuda and T. Tuda, Nucl. Fusion in press.

3] K.Itoh, T. Tuda and S. Inoue, J. Phys. Soc. Japan 48 (1980) 258.

4] W. M. Tang, Nucl. Fusion 18 (1978) 1089.

5] W. Horton Jr., R. Estes, H. Kwak and DukIn Choi, Phys. Fluids 21 (1978) 1366.

6] S. Inoue, K. Itoh and S. Yoshikawa, J. Phys. Soc. Japan 49 (1980) 367.

7] J. W. Connor, R. J. Hastie and J. B. Taylor, Proc. R. Soc. A365 (1979) 1.

8] R. J. Hastie, K. W. Hesketh and J. B. Taylor, Nucl. Fusion 19 (1979) 1223.

9] K. W. Hesketh, Nucl. Fusion 20 (1980) 1013.

10] C. Z. Cheng and L. Chen, Phys. Fluids 23 (1980) 1770.

11] L. Chen and C. Z. Cheng, Phys. Fluids 23 (1980) 2242.

12] D. W. Ross and S. M. Mahajan, Phys. Rev. Lett. 40 (1978) 324.

13] K. T. Tsang, P. J. Catto, J. C. Whitson and J. Smith, Phys. Rev. Lett. 4- (1978) 327.

14] A. Jennings, Matrix Computation for Engineers and Scientists, (Wiley, New York/London) Chap.5, p 145.

15] T. Tsunematsu, T. Takeda, T. Matsuura, G. Kurita and M. Azumi, Comp. Phys. Commun. 19 (1980) 179.

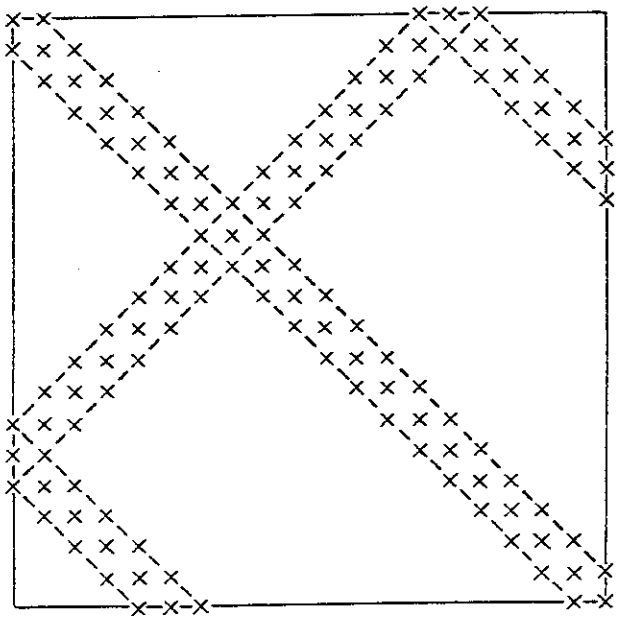

Fig.1.a Matrix structure of Eq.(3) for N = 20 and n = 15. Only nonzero elements are shown by the symbol x.

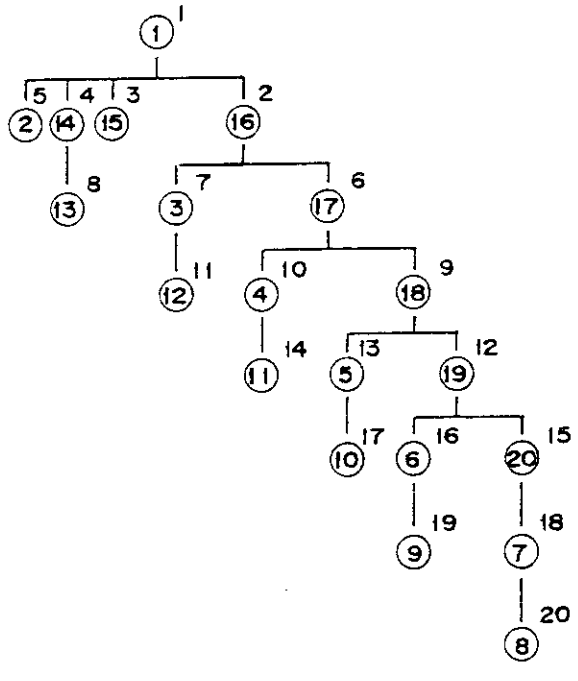

Fig.1.b Graphical representation of the post-order rule of matrix renumbering.

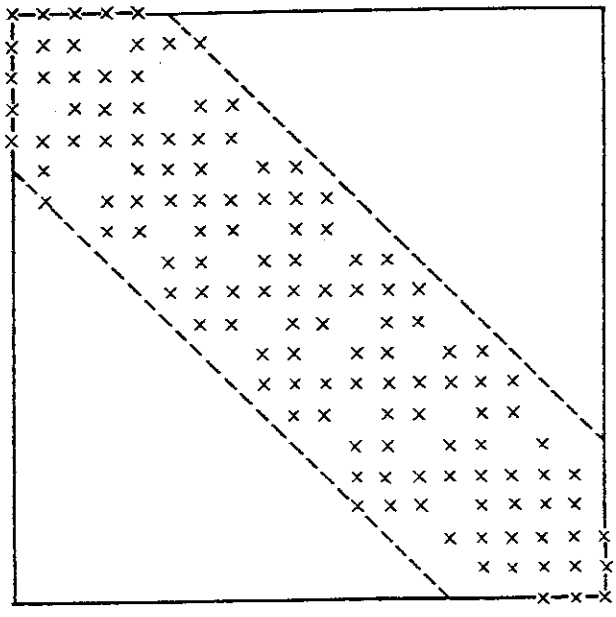

Fig.1.c Matrix structure after renumbering. The band width of the matrix is reduced to five.

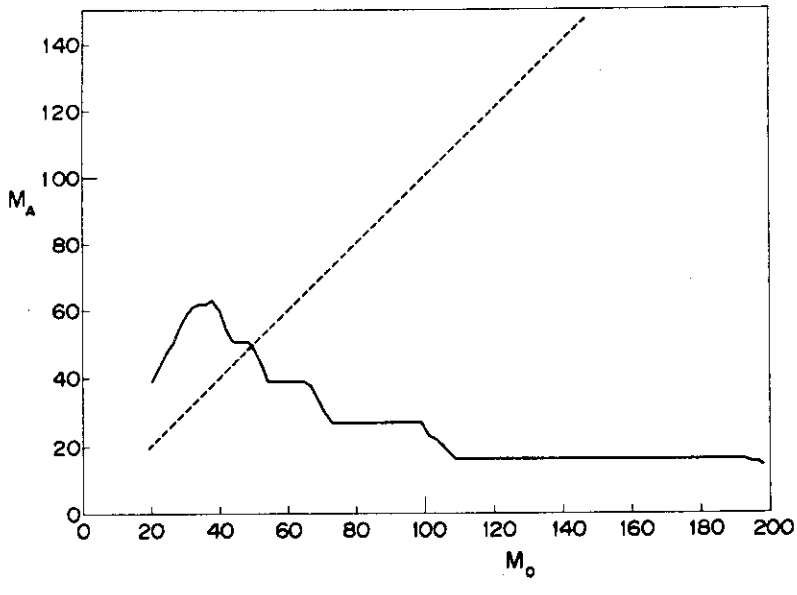

Fig.2 Band width after renumbering M_A vs. band width of the original matrix M_0 for the case of N = 200. The dotted line is $M_A = M_0$. Renumbering is profitable for $M_A \geq 50$.

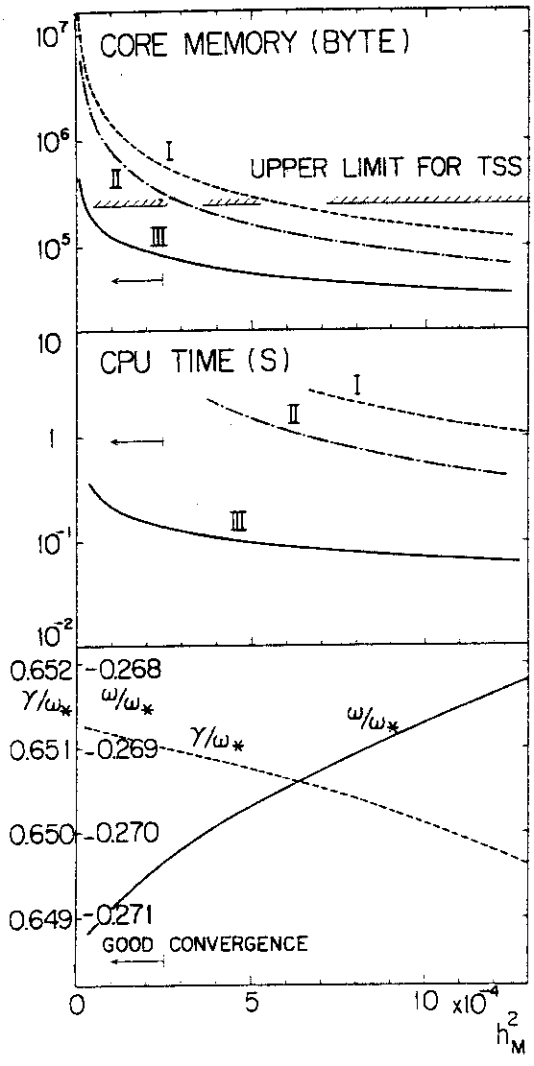

Fig.3 Core Memory (byte) (Fig.(3.a)) and CPU time (s) (Fig.(3.b)) necessary to compute $D(\omega)$ by FACOM M-200. (I) and (II) are the cases of LDU decomposition without and with use of the band structure, respectively. (III) is the case of the renumbered matrix. $h_M = h/(\kappa L_s)$ and h is mesh size. The truncation length $Nh = \kappa L_s$ is fixed. The shaded line (//////////) in Fig.(3.a) indicates the upper limit of core memory for TSS. The convergence curves of $\omega = \mathrm{Re}(\omega)$ and $\gamma = \mathrm{Im}(\omega)$ are shown by solid and dotted lines (Fig.(3.c)). The necessary mesh sizes to get 'good convergence' are also shown.

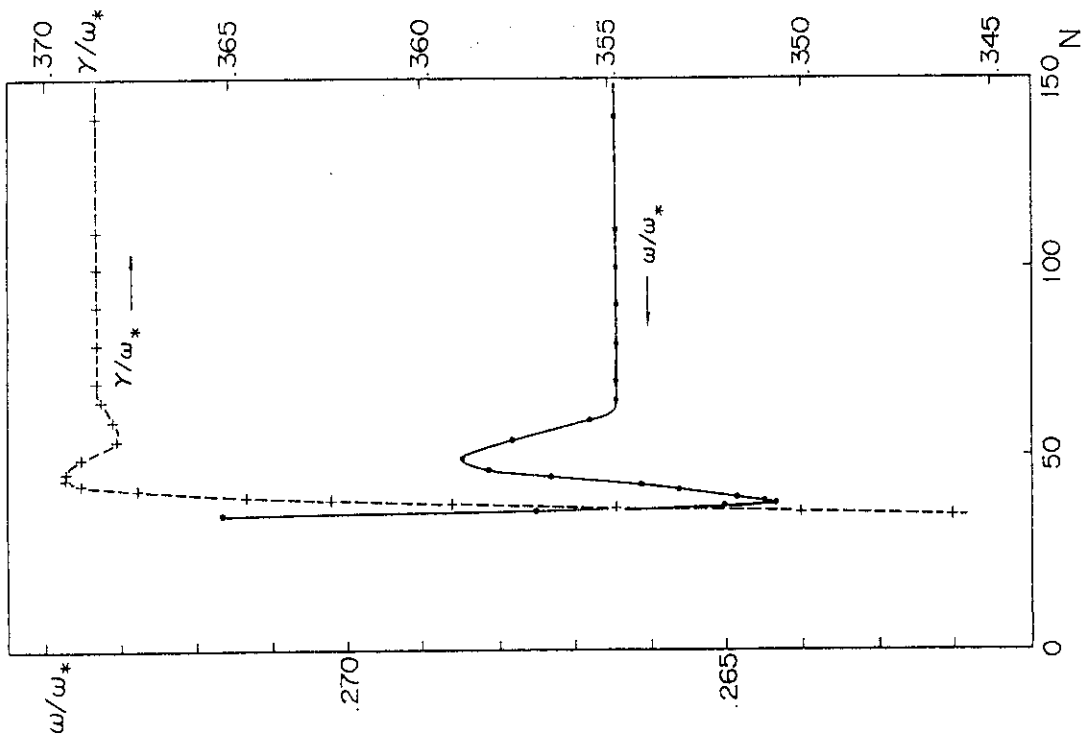

Fig.4.b The convergence curves when the truncation length is varied and the mesh size,h, is fixed to $h = 1.04\times10^{-2}\kappa L_s$.

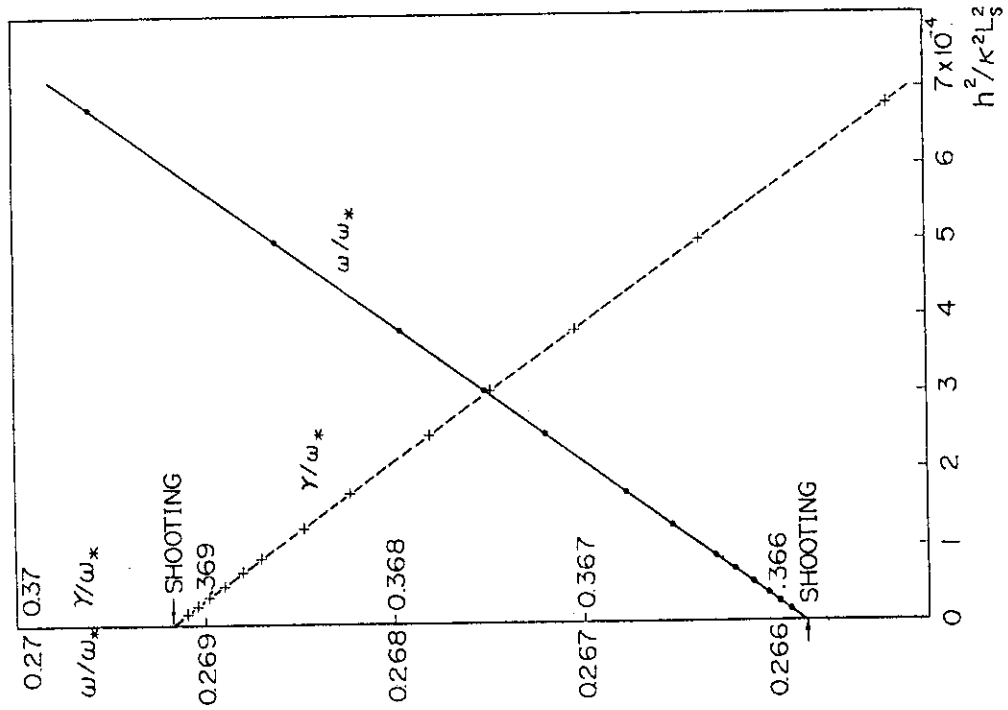

Fig.4.a The convergence curves of $\omega = \mathrm{Re}(\omega)$ (solid line) and $\gamma = \mathrm{Im}(\omega)$ (dotted line) for the case of the fluid limit ; $s = 1$, $k\rho_i = 0.2$, $q = 3.2$, $\tau = 1$, $\varepsilon = 0.1$ and $\Delta = 5$. The truncation length is fixed as $Nh = \kappa L_s$.

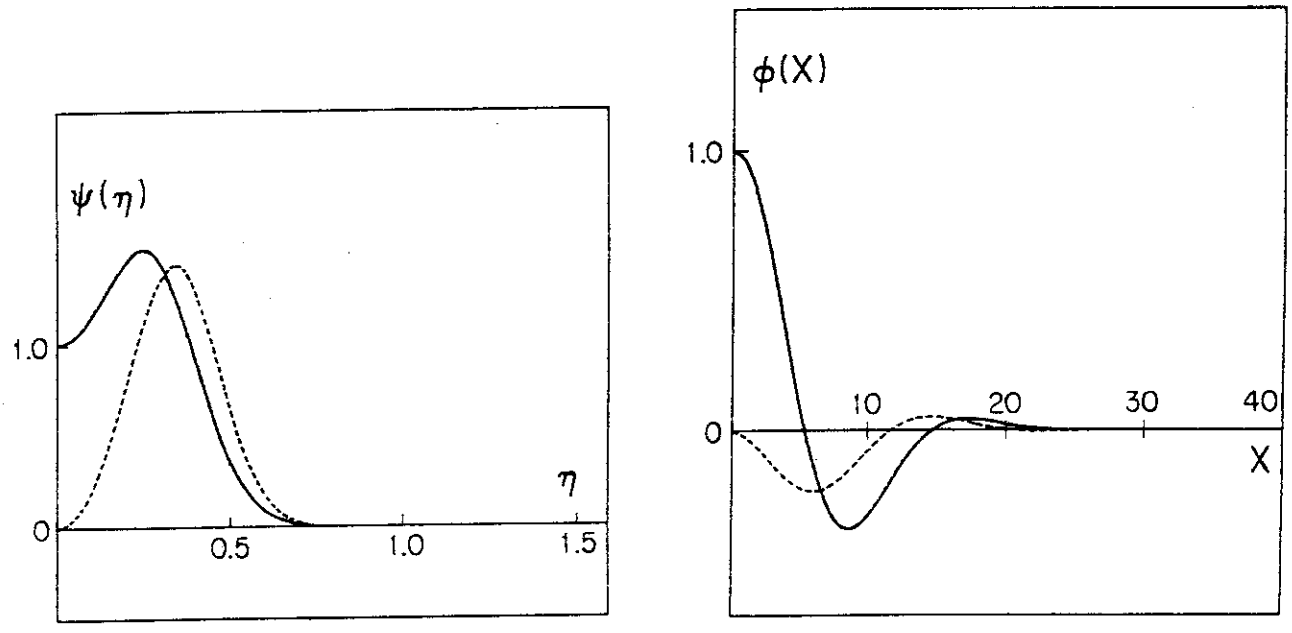

Fig.5 Eigensolution $\psi(\eta)$ obtained from the shooting method (Fig.5.a) and its Fourier transformation $\phi(x)$ (Fig.5.b). The solid and dotted lines indicate the real and imaginary parts of the solution, respectively.

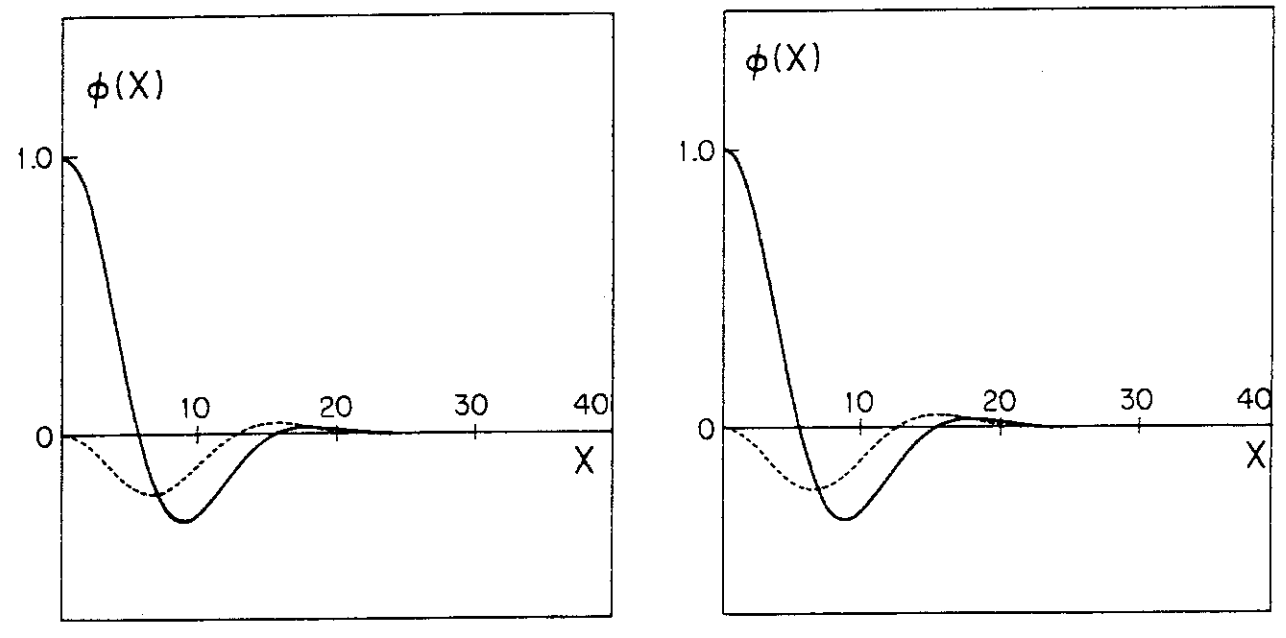

Fig.6 Eigensolutions obtained from the matrix method for the cases of (a) $h = 2.2\times10^{-2}\kappa L_s$ and (b) $h = 5.04\times10^{-3}\kappa L_s$.

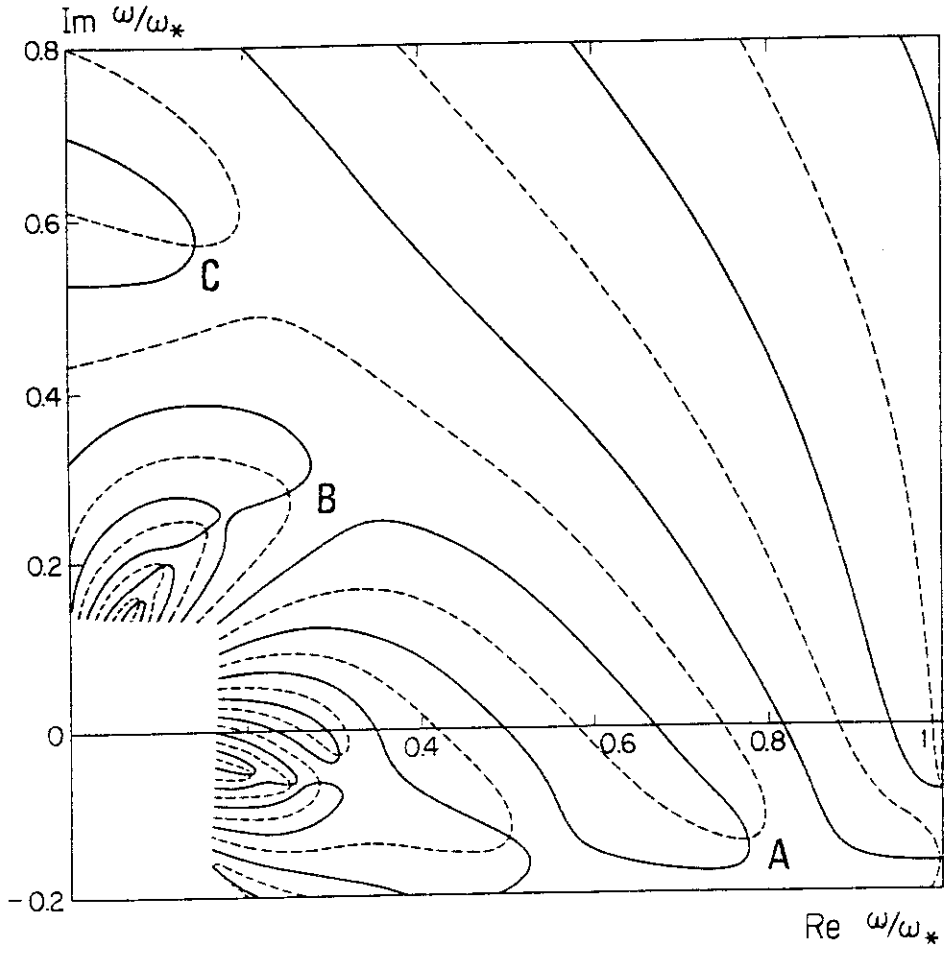

Fig.7 Contour map of $ReD(\omega) = 0$ (solid line) and $ImD(\omega) = 0$ (dotted line). Parameters are same in Figs.4. The crossing points A, B and C denote the eigenvalues belonging to the A, B and C branches, respectively.

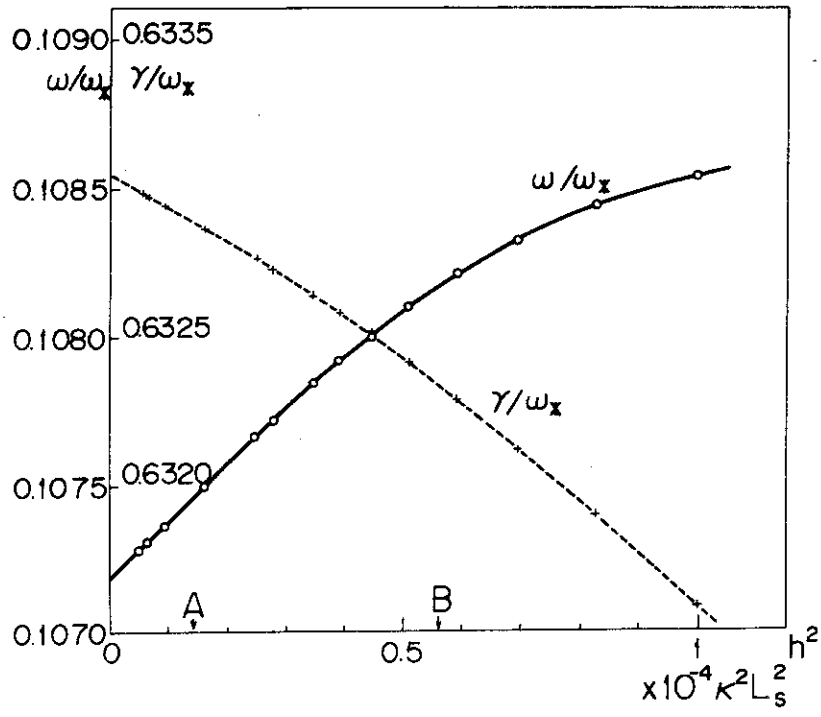

Fig.8 Convergence curves of the eigenvalue belonging to the C branch in Fig.7, where the parameters are : $q = 5$, $k\rho_i = 0.2$, $\tau = 1$, $s = 1$ and $\varepsilon = 0.1$. The point A denotes such a mesh size as $k_{//}(h_A)v_e/\omega \simeq 1/4$, and B denotes $k_{//}(h_B)v_e/\omega \simeq 1/2$.

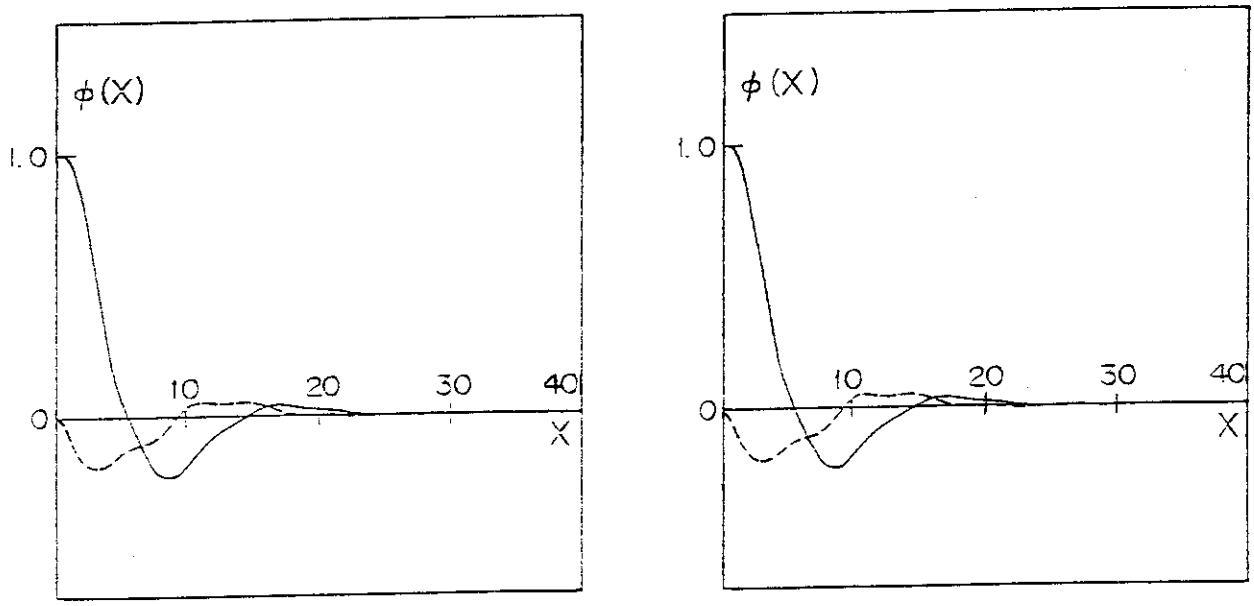

Fig.9 Eigensolutions for $h = 10^{-2}\kappa L_s$ (Fig.9.a) and $h = 0.25\times10^{-2}\kappa L_s$ (Fig.9.b) . Almost no difference is seen.